Journal of Al-Azhar University Engineering Sector

Vol. 20, No. 76, July 2025, 834-854

ASSESSING CLIMATE CHANGE PROJECTION IMPACTS ON PRECIPITATION IN THE BLUE NILE BASIN USING Reg-CM4 SIMULATIONS

Dina I. Youssef, [1,*], Sohier A. Mansour[2], Nabil M. Anwar[1]

[1] National Water Research Center, Ministry of Water Resources and Irrigation, Qalyubia, 13621, Egypt.

[2] Sanitary & Environmental Eng. Dept., Faculty of Engineering at Mataria, Helwan University, Cairo, Egypt.

* **Correspondence**: Eng.dinamo2010@gmail.com

Citation:

D. I. Youssef, S. A. Mansour, N. M. Anwar, "Assessing climate change projection impacts on precipitation in the Blue Nile Basin using Reg-CM4 simulations", Journal of Al-Azhar University Engineering Sector, vol. 20, pp. 834 - 854, 2025.

Received: 10 February 2025

Revised: 20 April 2025

Accepted: 10 May 2025

Doi: 10.21608/auej.2025.359285.1777

ABSTRACT

The Blue Nile Basin (BNB) is a crucial water resource for Ethiopia, Sudan, and Egypt, making it essential to assess climate change impacts on precipitation for effective water management. This study evaluates future precipitation changes using regional climate projections from the CORDEX-CMIP5 dataset with the RegCM4.3 model under RCP2.6 and RCP8.5 scenarios for two periods: 2041–2070 and 2071–2100. Bias correction was applied using a linear function based on historical simulations (1981–2005). The study analyzed seasonal precipitation distribution, Z-score, and Precipitation Concentration Index (PCI). Results indicate an overall decline in annual precipitation under both scenarios, with the most significant reduction (-15%) projected for 2071–2100 under RCP8.5. Seasonal variations show a decline in Kiremt (rainy) and Belg (semi-rainy) seasons (-14%, -34%) under RCP8.5, while the Dry season (Bega) shows a slight increase (11%), suggesting potential shifts in seasonal hydrological patterns. The Z-score analysis indicates stable normal-year occurrences but an increase in dry years at the expense of wet years for most stations. SPCI values for Kiremt were mostly ‘uniform’ in the historical period but ranged from ‘uniform’ to ‘moderate’ in future projections. Annual PCI values, which were ‘irregular’ to ‘strongly irregular’ historically, show a tendency toward more ‘strongly irregular’ values in the future. Overall, the study concludes that precipitation patterns in the BNB will change, increasing seasonal variability. Future research should refine climate projections with updated models and integrate socio-economic factors to enhance adaptation strategies and mitigate climate change impacts.

KEYWORDS: Blue Nile Basin, climate change, Reg-CM4.3, CORDEX-CMIP5, PCI.

تقييم تأثير التغيرات المناخية على معدلات الهطول المطرى في حوض النيل الأزرق باستخدام النموذج المناخى الإقليمى Reg-CM4

دينا إبراهيم يوسف ١، *، سهير أحمد منصور٢، نبيل محمد أنور١

١ معهد بحوث التغيرات المناخية وآثارها البيئية، المركز القومى لبحوث المياه، وزارة الموارد المائية والرى، القليوبية،١٣٦٢١، مصر.

٢ قسم الهندسة الصحية والبيئية، كلية الهندسة بالمطرية، جامعة حلوان، القاهرة، مصر.

***البريد الالكتروني للباحث الرئيسي:** Eng.dinamo2010@gmail.com

الملخص

يعد حوض النيل الأزرق (BNB) موردًا مائيًا بالغ الأهمية لكل من إثيوبيا والسودان ومصر، مما يجعل من الضروري تقييم تأثيرات التغير المناخي على الهطول المطري لضمان إدارة فعالة للموارد المائية. تهدف هذه الدراسة إلى تقييم التغيرات المستقبلية في بيانات الأمطار المستخرجة من مجموعة بيانات CORDEX-CMIP5 من النموذج المناخى الإقليمى RegCM4.3 وفقًا للسيناريوهات المناخية RCP8.5 -RCP2.6 خلال فترتين مستقبليتين ٢٠٤١–٢٠٧٠، ٢٠٧١–٢١٠٠ تم تطبيق تصحيح الانحياز باستخدام دالة خطية استنادًا إلى عمليات المحاكاة التاريخية للفترة من ١٩٨١ حتى ٢٠٠٥. شملت التحليلات توزيع الأمطار الموسمي، ومؤشر Z، ومؤشر تركيز الأمطار (PCI) موسميًا وسنويًا. تشير النتائج إلى ميل عام نحو ظروف أكثر جفافًا في الأمطار السنوية ضمن كلا السيناريوهين، حيث بلغ أقصى نسبة تغيير حوالى (-١٥٪) خلال الفترة ٢٠٧١–٢١٠٠ وفقًا لسيناريو RCP8.5 . كما أظهرت التغيرات الموسمية انخفاضًا في موسمي كيرِمت (المطير) وبِلْج (شبه المطير) بنسبة -١٤٪ ، -٣٤٪ على التوالي تحت السيناريو المتشائم، في حين شهد موسم بيجا (الجاف) زيادة طفيفة بنسبة ١١٪، مما يشير إلى تغيّرات محتملة في الأنماط الهيدرولوجية الموسمية. أظهر تحليل قيم مؤشر Z استقرارًا في تكرار السنوات العادية، مع زيادة في عدد السنوات الجافة على حساب السنوات الرطبة في معظم المحطات. أما مؤشر تصنيف شدة الامطار SPCI لموسم كيرِمت، فقد كان "uniform" خلال الفترة التاريخية، لكنه تراوح بين " uniform " إلى" moderate " في الإسقاطات المستقبلية. في المقابل، أظهرت القيم السنوية لـ PCI، والتي كانت تتراوح بين " irregular" إلى" strongly irregular" تاريخيًا، ميلًا نحو مزيد من " strongly irregular" في المستقبل. بشكل عام، تستنتج الدراسة أن أنماط الهطول المطري في حوض النيل الأزرق ستشهد تغيرات مستقبلية مع زيادة التباين الموسمي. لذا، ينبغي أن تركز الأبحاث المستقبلية على تحسين الإسقاطات المناخية باستخدام نماذج محدثة، يستخدم فيها دمج العوامل الاجتماعية والاقتصادية لتعزيز استراتيجيات التكيف والتخفيف من الآثار السلبية لتغير المناخ.

الكلمات المفتاحية : حوض النيل الأزرق، التغير المناخي، Reg-CM4.3، CORDEX-CMIP5، PCI.

1. INTRODUCTION

Climate change is increasingly recognized as a major threat to global water resources, particularly in river basins that are highly sensitive to shifts in temperature and precipitation patterns. Across the world, changes in climate are altering hydrological cycles, leading to more frequent and intense floods, prolonged droughts, and variability in river flows [1]. These effects are especially pronounced in developing regions where adaptive capacity is limited [2]. In Africa, many transboundary river basins face mounting pressure as climate variability threatens agricultural productivity, water security, and energy generation [3].

Among these, the Blue Nile Basin stands out as a critical water source shared by Ethiopia, Sudan, and Egypt, contributing approximately 60% of the Nile River's total flow [4]. Its waters are vital for agriculture, hydropower, and domestic use, supporting millions of people downstream [5]. However, the basin is highly vulnerable to climate change. Altered seasonal flow regimes driven by rising temperatures and shifting precipitation patterns may reduce water availability [6]. Moreover, an increase in extreme weather events, such as floods and droughts, complicates water management efforts and heightens the risk of food insecurity [7]. Addressing these complex challenges will require adaptive strategies and enhanced regional cooperation to ensure the sustainable management of the basin's resources [8].

Climate change is becoming of great concern to many countries in the world, with special focus on its potential impacts on precipitation and on water resources management planning. The Inter-governmental Panel on Climate Change (IPCC) issued future projection scenarios for greenhouse gas emissions that are mainly responsible for climatic changes, which varied from the most optimistic scenario of RCP2.6 for curbing down the CO_2 emissions, to the most pessimistic scenario of RCP8.5. General Circulation Models (GCMs) have been used [9], with downscaling using Regional Climate Models (RCMs) to higher spatial resolutions [10] by many institutions to develop dynamic projections for regional climates in many parts of the world until the year 2100. The Intergovernmental Panel on Climate Change (IPCC) Fourth Assessment Report highlights the challenges faced by water resource managers in the region, including excessive precipitation, altered seasonal flow patterns, and the increasing frequency and severity of floods and droughts [11]. These challenges underscore the need for accurate climate projections to support sustainable water resource development and management in the Blue Nile Basin.

Multiple studies have assessed the performance of Regional Climate Models (RCMs) and their driving Global Climate Models (GCMs) across various basins in Ethiopia, highlighting significant spatial and temporal variability in model accuracy. One study evaluated 14 CORDEX-Africa RCMs over the Katar Watershed, revealing diverse model performances and limitations due to inherent biases, localized focus, and omission of future scenarios [12]. Another assessment of five CORDEX RCMs in the Arsi Zone found that ensemble means were more effective in simulating temperature than precipitation, with performance highly sensitive to topography [13]. A separate analysis of five RCMs driven by various GCMs over the Omo Gibe River Basin emphasized the need for ensemble means and bias correction due to overestimated return periods of extreme events [14]. Other studies reported significant performance variability in CORDEX RCMs across the Wabi Shebele and Gidabo river basins, noting that ensemble means do not always outperform individual models and highlighting the importance of bias correction [15, 16]. Observational data from 1950–2018 indicated rising temperatures and declining precipitation trends in the Blue Nile Basin, along with increasing droughts linked to ENSO events [17, 18]. One projection study using the Rossby Centre Atmospheric Model (RCA) driven by four GCMs under RCP4.5 and RCP8.5 scenarios projected significant temperature rises, up to 54% streamflow reduction, and major seasonal water balance shifts [19]. Another analysis using ensembles of five CMIP5 GCMs and ten CORDEX RCMs found improved performance with bias correction but continued difficulty in simulating extremes, projecting increased annual discharges and seasonal shifts [20]. Research on different convective schemes in RegCM4 over West Africa recommended the Emanuel scheme for its reduced temperature and precipitation biases [21]. Further evaluations using dynamically downscaled CMIP5 models over the Upper Blue Nile noted precipitation biases and projected streamflow reductions due to climate change [22, 23]. A comparative study based in the U.S. using ten statistically downscaled GCMs projected increased drought intensity and seasonal hydrological shifts, identifying GCM uncertainty as a dominant challenge [24]. These findings collectively underscore the necessity of model selection, bias correction, and ensemble approaches tailored to regional conditions for reliable climate impact assessments.

Many studies have successfully applied the ICTP-RegCM4 Regional Climate Model to the Blue Nile Basin (BNB) over various periods. The model was applied to the BNB for the period 1982 to 2009 in one study [11], and another also used the same duration [25]. A separate application of RegCM4 covered the period from 1981 to 2005 [26], and the same period was used in a previous study by the current authors [27]. One study examined CORDEX-RegCM4.3 hindcast simulation results for precipitation over the BNB, focusing on six selected meteorological stations: Roseires in Sudan, and in Ethiopia: Gonder and Bahr Dar at Lake Tana in the north, Kembolcha in the east, Debre Markos in the middle, and Nekemte in the south [27]. Bias correction and statistical evaluations (PDF, CDF, NSE, bias, RMSE) were applied to the simulation outputs, showing good agreement with observational data and supporting the recommendation to use CORDEX-RegCM4.3 projections for the BNB up to the year 2100 [27].

The objective of the current study is to assess the impacts of future climatic changes on precipitation in the Blue Nile Basin using CORDEX-RegCM4.3 future projection simulation results for future durations of (2041-2070 & 2071-2100), as compared to WATCH historical observation data in the duration of (1981-2005). Average seasonal precipitation is calculated to evaluate on the spatial distribution of precipitation for the three main seasons on the Blue Nile basin.

2. DATA AND METHODOLOGY

To analyze spatial and temporal variability, seasonal mean precipitation values were extracted to compare future simulations with historical observations. The standardized Z-score method was applied to classify interannual precipitation variability into wet, normal, and dry years. Additionally, the Precipitation Concentration Index (PCI) and its seasonal variant (SPCI) were computed to examine the distribution and concentration of monthly precipitation both annually and seasonally. These indicators help in the assessment of temporal distribution of precipitation, which can be used for flood/drought risk assessment and water management planning [28, 29].

2.1. The Study Area

The Blue Nile is a major tributary in the Nile Basin and is a major contributor to water resources in Ethiopia, Sudan and Egypt. The Blue Nile Basin (BNB) catchment area is approximately 310,000 km², with the river total length is about 1,450 km, of which 800 km in Ethiopia and 650 km in Sudan, where it discharges into the main Nile River near Sudan capital city of Khartoum [30]. Originating from Lake Tana in Ethiopia, the Blue Nile River flows southward, then westward through Ethiopia, and eventually northwest into Sudan. Near Khartoum, Sudan, the Blue Nile converges with the White Nile, at start of the main Nile River. The Blue Nile River Basin catchment area is approximately 310,000 km², located between latitudes 9°N and 16°N and longitudes 32°E and 40°E [31].

The Blue Nile Basin is characterized by significant topographical variations, with elevations ranging from approximately 380 m near Khartoum to over 4,200 m above mean sea level (M.S.L.) in the Ethiopian highlands [32]. The Blue Nile River stream-flow is predominantly influenced by the summer monsoon, which occurs primarily between July and October, and generates over 80% of its annual discharge, which greatly participates to water resources in Ethiopia, Sudan and Egypt [33].

The spatial distribution of precipitation in the BNB is diverse, as annual precipitation exceeds 1,200 mm in the Ethiopian highlands, and decreases to less than 400 mm in the Sudanese lower lands [34]. Temporal variability of yearly total precipitation varies significantly, ranging from 50 to 2000 mm/year, which may experience successive years of prolonged flood/drought durations [35]. The Inter-Tropical Convergence Zone northward movement during the Boreal Summer months is the main climatic driver of flood season precipitation, in addition to air inflows from the Gulfs of Congo and Guinea, the Sahel region, the Mediterranean and Red Seas, the Arabian Sea and the Gulf of Aden, and the Indian Ocean [36].

Precipitation in the BNB is sub-divided into 3 seasons: (I) The Belg Season (Semi-Rainy Season: February to May), with monthly averages ranging from 50 to 100 mm. (II) The Kiremt Season (Rainy Season: June to September), with average monthly precipitation often exceeding 200 mm in many areas. (III) The Bega Season (Dry Season: October- January), with monthly averages often below 20 mm [37].

Fig. 1 shows the location of the Blue Nile Basin as part of the Nile Basin in east Africa. In addition, it displays land elevation where higher lands are in the southern Ethiopian part of the basin and lower lands are in the Sudanese part at the North. Also, it shows the locations of the selected 6 meteorological observation stations used in the current study: (1) Roseires in Sudan, and in Ethiopia: (2) Gonder & (3) Bahr Dar at Lake Tana; in the Basin north, (4) Kembolcha in the east, (5) Debre Markos in the middle, and (6) Nekmte in the south.

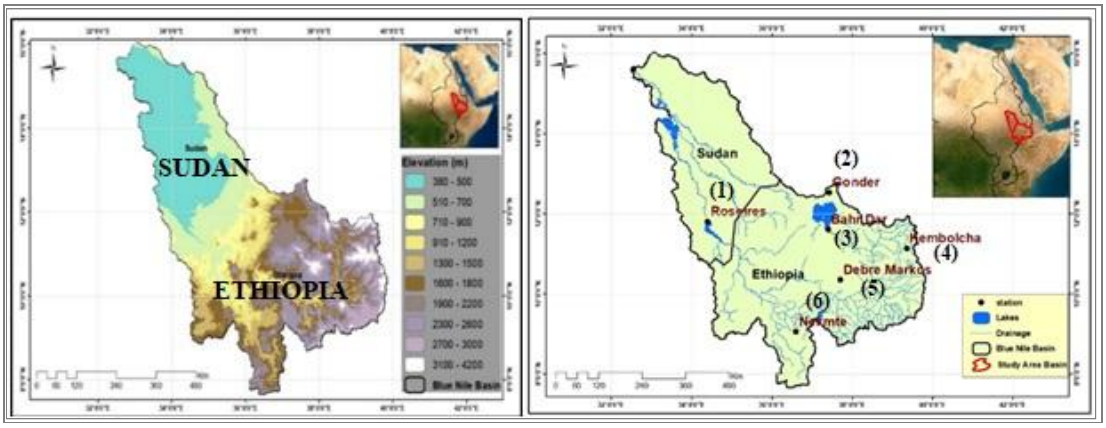

Fig. 1: Location, Topography & Catchment area of the Blue Nile Basin with studied locations

2.2. Historical Precipitation Observation Data (1981 – 2005)

The current study used daily observation precipitation data from WATCH data set for the Blue Nile Basin (BNB) and at the selected stations for the duration of (1981-2005). Precipitation data of

"WATCH-WFDEI" (WATCH: Water and Global Change; WFDEI: WATCH Forcing Data using the ERA-Interim reanalysis), was downloaded from the website (https://rda.ucar.edu/datasets/d314002/; DOI: 10.5065/486N-8109). ERA-Interim is atmospheric reanalysis project which assimilated historical atmospheric observational data for an extended period of time. WFDEI data is at the resolution of 0.5° x 0.5° and is Bias-corrected for precipitation using data from the Global Precipitation Climatology Centre (GPCC), which is based on in-situ observations from rain gauge networks.

A previously conducted study used the same precipitation observation data employed in the current research (WATCH dataset; from 1981 to 2005) for BNB, along with data from six meteorological stations as shown in **Fig. 1** [27]. In addition, the CHIRPS dataset (Climate Hazards Center InfraRed Precipitation with Station data; https://www.chc.ucsb.edu/data/chirps) was utilized, and the results indicated that the two datasets were nearly identical [27]. The WATCH dataset was also used for bias correction of RegCM4 hindcast simulations, with the period 1975–1990 used for calibration and 1991–2005 for validation [27].

2.3. Future Projection Model Simulations (2041 – 2070 & 2071 – 2100)

The current study used the regional climate model RegCM4.3 future projection simulation results of CORDEX-CMIP5 project (CORDEX: "Coordinated Regional Climate Downscaling Simulation"; CMIP5: "Coupled Model Inter-comparison Project Phase 5"; https://cordex.org/). Selected CORDEX-RegCM4.3 simulations covered the future periods of 2041-2070 & 2071-2100 under IPCC RCP2.6 & RCP8.5 for most optimistic and most pessimistic future emission scenarios, respectively. RegCM4-CORDEX simulations are done at the resolution of 0.22° x 0.22° (approximately at 25 km x 25 km), and are driven by General Circulation Model (GCM) called MPI-M-MPI-ESM-MR, which was also evaluated in our previous study [27].

Bias-correction of future-projection data

This paper performed bias correction to future projection simulations using the linear equation as shown in Eq.1 that was used in the study [27] for CORDEX-RegCM4.3 hindcast simulations of the duration from 1981 to 2005:

$$P_{cor,m,d} = P_{raw,m,d} \text{ x } \left(\frac{\mu, \left(P_{obs.,m}\right)}{\mu \ \left(P_{raw,m}\right)} \right) \tag{1}$$

Where:

$P_{cor,m,d}$ corrected value of precipitation monthly or daily.
$P_{raw,m,d}$ raw value of precipitation monthly or daily.
$P_{obs.,m}$ Observed value of precipitation monthly or daily.
μ symbolizes the operator of expectation (e.g., $\mu\ (P_{obs})$),
m symbolizes the average amount of precipitation observed during a specific month (m).

The WATCH dataset record from 1979 to 1990 was used for calibration, and the period from 1991 to 2005 was used for validation in the bias correction of RegCM4 simulation results for the same time period [27]. The calibrated parameter values derived from this analysis were adopted in the current study to perform bias correction on future projection model simulations for the periods 2041–2070 and 2071–2100 [27].

2.4. Z-Score Test (for Wet, Normal and Dry Years)

The Z-score is a statistical metric widely employed in precipitation studies to evaluate anomalies and/or the deviations from long-term mean precipitation patterns. By standardizing precipitation data, the Z-score facilitates the classification of climatic conditions, such as droughts and floods, while enabling the analysis of climate variability over different regions and temporal scales [38], calculated as follows in Eq. 2:

$$Z = \frac{x - \mu}{\sigma} \tag{2}$$

Where:

Z is the score for each year in the studied duration,
x is the yearly precipitation of that year,
μ is the annual mean precipitation of the studied duration,
σ is the annual precipitation standard deviation of the studied duration.

Years of the studied duration are classified into dry, normal and wet for $Z < -0.5$, $-0.5 < Z < 0.5$, and $Z > 0.5$; respectively [38]. The advantage of using the standardization procedure is that it aids in discerning normal and typical values and is symmetrical for the occurrence of wet, normal and dry events [39].

2.5. Annual/Seasonal Precipitation Concentration Indexes (PCI/SPCI)

The Precipitation Concentration Index (PCI) is a statistical measure used to evaluate the temporal distribution and variability of precipitation within a specific period, such as monthly, seasonal, or annual scales. This index provides insights into the degree of uniformity or irregularity in precipitation patterns, which is crucial for understanding hydrological processes, climate variability, and water resource management [40].

The annual PCI is calculated according to Equations 3 [41]:

$$\mathrm{PCI_{annual}} = \frac{\sum_{i=1}^{12} P_i^2}{(\sum_{i=1}^{12} P_i)^2} \mathrm{x}100 \tag{3}$$

Where:

P_i is the monthly precipitation during the i^{th} month.

For the 3-month Seasonal Precipitation Concentration Index (SPCI), the right-hand side of the equation was divided by 4, corresponding to one-fourth of the year [42]. Similarly, for the 4-month seasons used in the current study ($1/3^{rd}$ of the year), Equation 4 is expressed accordingly [40]:

$$\mathrm{SPCI_{seasonal}} = \frac{\sum_{i=1}^{4} \mathrm{P_i^2}}{(\sum_{i=1}^{4} \mathrm{P_i})^2} \mathrm{x} \frac{100}{3} \tag{4}$$

The PCI and SPCI values are categorized into classes that describe the concentration of precipitation distribution [42]:

- **<10%**: Uniform precipitation distribution (low precipitation concentration).
- **11-15%**: Moderate precipitation distribution.
- **16-20%**: Irregular precipitation distribution.
- **>20%**: Strong irregularity in precipitation distribution (high precipitation concentration).

Uniform (or low) precipitation concentration distribution means that the total amount of precipitation is well distributed over the months of the studied period. Meanwhile, irregular precipitation is concentrated with higher values in fewer months of the studied duration, while the other months experience less precipitation values.

3. RESULTS AND DISCUSSION

3.1. Spatial Distribution of Seasonal Precipitation in the Blue Nile Basin

The belg season (semi rainy season, February to May)

Fig. 2 illustrates the spatial distribution of average precipitation (mm) in The Belg Season (semi-rainy) under different climate scenarios (RCP2.6 and RCP8.5) compared to the historical period (1981-2005). Average historical precipitation in this season ranged from 2 to 504 mm in the Blue Nile Basin (BNB). Meanwhile, future projection average precipitation for the duration (2041-2070) ranged from 2 to 496 & 0 to 418 mm, and for the duration (2071-2100) ranged from 3 to 498 mm & 0.5 to 352 mm for RCP2.6 & RCP8.5; respectively.

The historical data indicate relatively higher precipitation in the southern region, decreasing northward. In general Future projections indicate decreasing in precipitation, especially under the high emissions scenario (RCP8.5), with the most significant trend towards drought observed in the late 21st century (2071–2100). While RCP2.6 exhibits a less severe decline, it still shows a shift towards drier conditions in several areas. The increasing dominance of blue shades, representing lower precipitation, suggests a heightened risk of drought, which could have significant implications for water resources, agriculture, and ecosystem sustainability in the region.

The kiremt season (rainy season, June to September)

The spatial distribution of average precipitation (mm) in The Kiremt Season (rainy) for historical period (1981-2005) as compared to future projection simulation results for RCP2.6 & RCP8.5 emission scenarios in the future durations (2041-2070 & (2071-2100) is shown in **Fig. 3**

In the upper part of **Fig. 3**, comparison of historical average precipitation to RCP2.6 & RCP8.5 scenarios for the duration (2041-2070) shows general decrease in future projection precipitation, with the RCP8.5 scenario slightly drier than the RCP2.6. The average precipitation in the historical data ranged from104 mm to 1480 mm across the basin. It is also observed that higher precipitation is concentrated in the central and southern parts of the basin, while the northern areas receive significantly less precipitation. In the future duration of (2041-2070) for the RCP2.6 scenario, lower precipitation zones (100-300, 300-500 & 500-700 mm) in the BNB north and middle expand further to the south, with larger expansion for the RCP8.5 scenario. The central and southern parts of the basin south and the southern tip (which received highest precipitation in the historical duration) showed some shrinkage in the areas of highest precipitation (900-1100 & 1100-1300 mm) in both scenarios, with larger shrinkage in the RCP8.5 scenario.

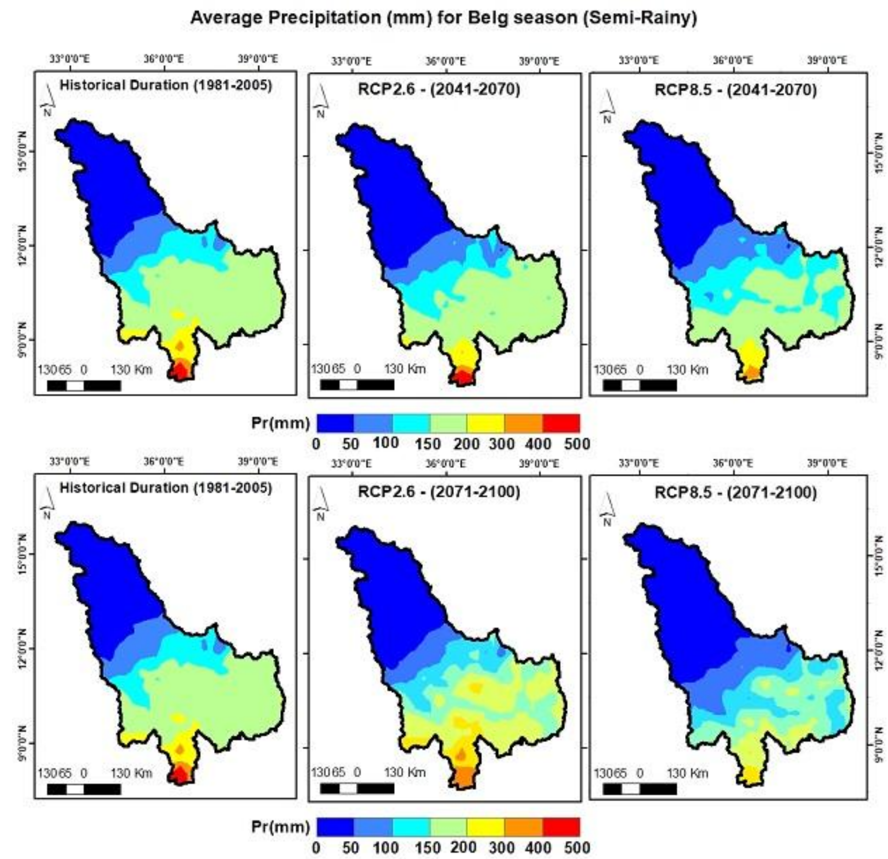

Fig. 2: Seasonal precipitation (mm) in Belg Season (semi-rainy season; February to May) for historical period (1981-2005) and two future durations (2041-2070) - (2071-2100) for two emission scenarios RCP2.6 & RCP8.5

In the lower part of the **Fig. 3**, by comparing the predicted precipitation with historical data, it showed a large decrease in future periods, with the RCP8.5 scenario drier than the RCP2.6. Similar to the projection of the (2041-2070) duration, there was southward expansion in the lower precipitation zones (100-300, 300-500 & 500-700 mm) in the BNB north and middle. Meanwhile, the central and southern parts of the basin south and the southern tip (which received highest precipitation in the historical duration) showed more shrinkage in the areas of highest precipitation (900-1100 & 1100-1300 & 1300-1500 mm) for both scenarios. However, there was larger shrinkage in these values in the RCP8.5 scenario, with disappearance of values in the ranges (1100-1300 & 1300-1500 mm) in the BNB southern tip.

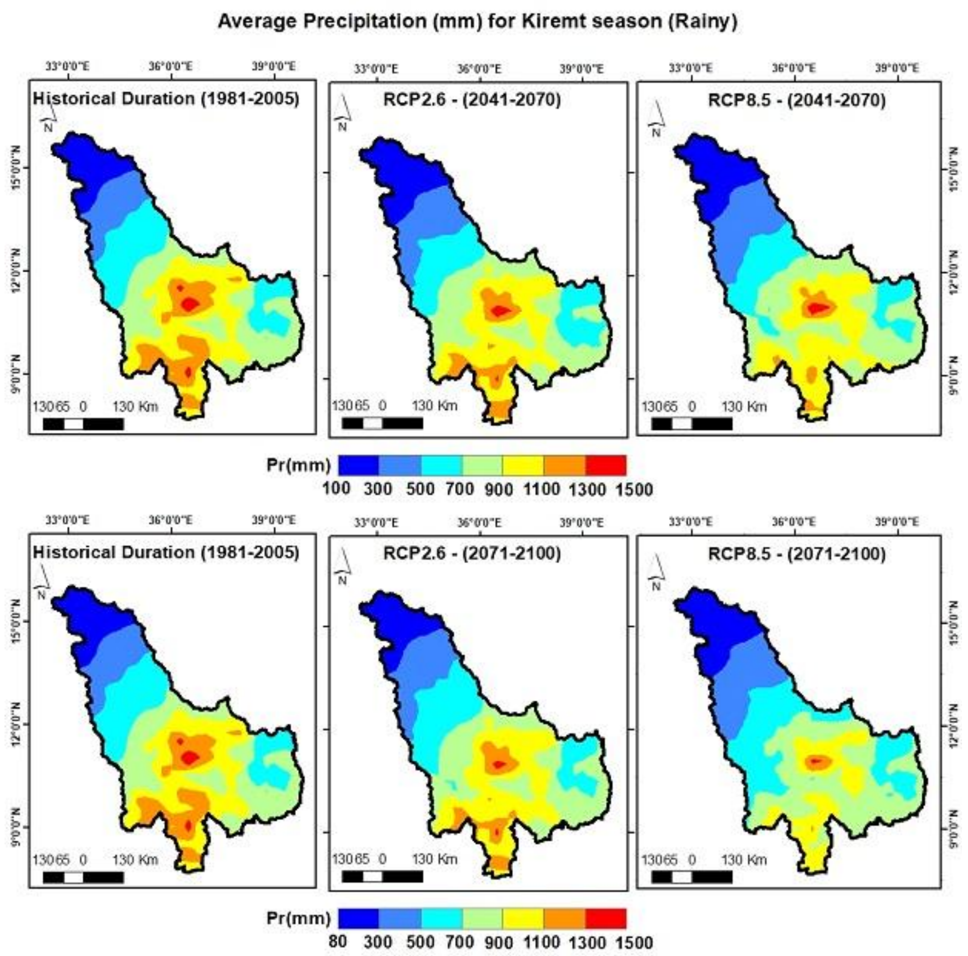

Fig. 3: Seasonal precipitation (mm) in Kiremt Season (rainy season; June to September) for historical period (1981-2005) and two future durations (2041-2070) - (2071-2100) for two emission scenarios RCP2.6 & RCP8.5

The bega season (the dry season, October to January)

Fig. 4 shows the spatial distribution of average precipitation (mm) for the Bega season (dry) in BNB based on historical data and future projections under the RCP2.6 and RCP8.5 emission scenarios for the two future periods.

Average historical observation precipitation in the drier season for the duration from 1981 to 2005 ranged from 4 to 300 mm all over the Basin (BNB). Meanwhile, future projection average precipitation for the duration (2041-2070) ranged (3 to 318 & 7 to 272 mm) and for the duration (2071-2100) ranged (8 to 312 mm & 6 to 317 mm)) for RCP2.6& RCP8.5; respectively.

The historical precipitation distribution shows higher value in the southern and central regions, while the northern areas remain significantly drier. Future projections indicate a general drying trend, particularly under the RCP2.6 scenario, where lower precipitation zones (0-50 mm and 50-100 mm) expand southward. The RCP8.5 scenario shows slightly higher precipitation compared to RCP2.6 but still exhibits a reduction in precipitation compared to historical data. The projected drying trend is more evident in the late-century period (2071-2100), with a noticeable shrinkage of higher precipitation zones (200-300 mm) in the southern regions, especially under RCP2.6.

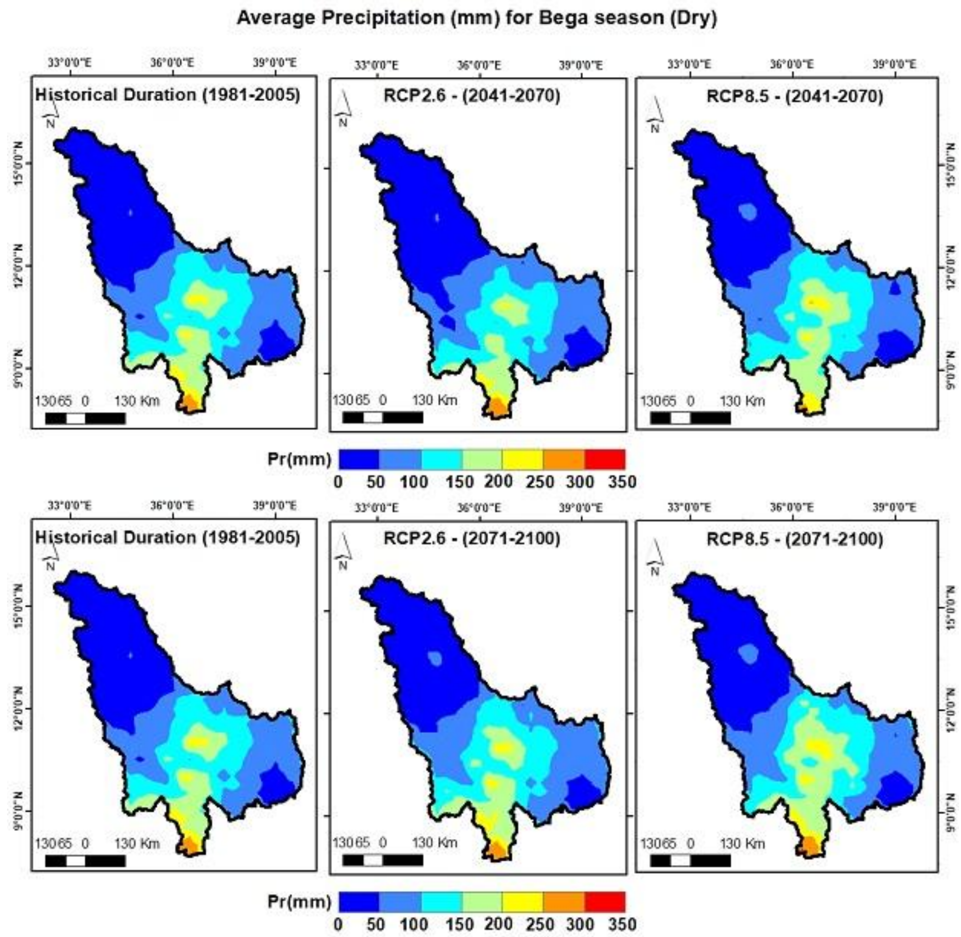

Fig. 4: Seasonal precipitation (mm) in Bega Season (dry season; October to Januar) for historical period (1981-2005) and two future durations (2041-2070) - (2071-2100) for two emission scenarios RCP2.6 & RCP8.5

3.2. Seasonal Precipitation at the Studied Meteorological Stations
The belg season (semi rainy)

Seasonal average precipitation (mm) for semi-rainy season "Belg" at the studied stations for historical period (1981 –2005) and the two future durations under scenarios RCP2.6 & RCP8.5, with percent change in future projection simulations is showed in **Table 1.**

The Table presents a comparative analysis of seasonal precipitation for the Belg season across six stations in the Blue Nile Basin, highlighting historical data (1981-2005) and projected changes under RCP2.6 and RCP8.5 scenarios for two future periods (2041-2070 and 2071-2100). A general decreasing trend in precipitation is observed across most stations, particularly under the RCP8.5 scenario, where reductions are more pronounced. Roseires Station exhibits the highest reduction, reaching -62.24% in 2071-2100 under RCP8.5. In contrast, Gonder and Bahr Dar stations show an increasing trend in RCP2.6 for 2071-2100, with precipitation increases of 20.35% and 11.85%, respectively. Similarly, Debre-Markos and Nekmte stations display slight increases under RCP2.6 (3.77% and 1.49%, respectively), indicating potential localized resilience to climate change. However, Kembolcha consistently experiences declining precipitation across all scenarios, suggesting heightened vulnerability. Overall, the projections indicate a future characterized by drier conditions, especially under RCP8.5, with potential implications for water availability and agricultural productivity in the basin.

Table 1: Average Seasonal precipitation (mm) for Belg season in Historical period and two future period under RCP2.6 & RCP8.5 scenarios, with percent change (% Decrease & % Increase)

No.	Stations*	Historical Observation Data (1981-2005) Prec. (mm)	(2041-2070) RCP2.6	(2041-2070) RCP8.5	(2071-2100) RCP2.6	(2071-2100) RCP8.5
			Prec. (mm) % Change		Prec. (mm) % Change	
1	Roseires	51.9	38.4 -26.01%	39.8 -23.31%	42.4 -18.30%	19.6 -62.24%
2	Gonder	131.2	117.05 -10.79%	107.8 -17.84%	157.9 20.35%	82.8 -36.89%
3	Bahr Dar	112.6	94.65 -15.91%	92.1 -18.18%	125.9 11.85%	81.9 -27.24%
4	Kembolcha	295.3	233.5 -20.93%	221.2 -25.09%	272.4 -7.75%	221.5 -24.99%
5	Debre-Markos	225.4	228.1 1.2%	178.7 -20.72%	233.9 3.77%	171.4 -23.96%
6	Nekmte	356.8	333.16 -6.63%	300.3 -15.84%	362.1 1.49%	250.3 -29.85%

* Station locations are shown in figure (1)

The Kiremt Season (Rainy Season)

Table 2 presents the seasonal average precipitation (mm) at Kiremt season (Rainy Season; June to September) at the stations for the three-time periods under RCP2.6 & RCP8.5 scenarios, with percent change.

The analysis of seasonal precipitation indicates a general declining trend in future projections compared to historical observations (1981–2005), particularly under the high-emission RCP8.5 scenario. Roseires, Gonder, Bahr Dar, and Nekmte stations show consistent decreases, with the most significant reductions at Gonder (-21%) and Nekmte (-19%) by 2071–2100 under RCP8.5. Conversely, Debre-Markos exhibits an increasing trend across all scenarios, with projected precipitation rising by up to +14% under RCP8.5. Kembolcha presents mixed trends, with both increases (+9%) and decreases (-11%) depending on the scenario and time period. These findings highlight spatial variability in future precipitation patterns, with potential implications for water resources and agriculture in the region.

Table 2: Average Seasonal precipitation (mm) for Kiremt season in Historical period and two future period under RCP2.6 & RCP8.5 scenarios, with percent change (% Decrease & % Increase)

No.	Stations	Historical Observation Data (1981-2005) Prec. (mm)	(2041-2070) RCP2.6	(2041-2070) RCP8.5	(2071-2100) RCP2.6	(2071-2100) RCP8.5
			Prec. (mm) % Change		Prec. (mm) % Change	
1	Roseires	579.9	564.8 -2.60%	529.3 -8.73%	565.5 -2.48%	511.6 -11.78%
2	Gonder	828.9	757.4 -8.63%	743.7 -10.28%	748.6 -9.69%	654.4 -21.05%
3	Bahr Dar	1066.1	994.8 -6.69%	1013.3 -4.95%	991.9 -6.96%	915.1 -14.16%
4	Kembolcha	651.0	579.9 -10.92%	682.5 4.84%	711.2 9.25%	645.7 -0.81%
5	Debre-Markos	926.5	960.7 3.69%	1034.8 11.69%	952.9 2.85%	1056.8 14.06%
6	Nekmte	1261.8	1194.1 -5.37%	1135.0 -10.05%	1210.7 -4.05%	1019.8 -19.18%

The Bega Season (Dry Season)

The projected seasonal average precipitation for the drier season (Bega) is presented in **Table 3.** The results indicate varying trends for the two projection periods (2041–2070 & 2071–2100) under scenarios RCP2.6 & RCP8.5 compared to historical period.

Roseires Station is projected to experience an increase in precipitation, ranging from +7% to +21%. Gonder Station shows mixed trends, with decreases of up to -6.5% under RCP2.6 and minor increases of up to +1% under RCP8.5. Bahr Dar Station exhibits contrasting trends, with reductions of up to -14% under RCP2.6 and increases reaching +18.5% under RCP8.5. Kembolcha predominantly shows a decline in precipitation of up to -12%, except for one scenario under RCP2.6, which predicts a +5% increase.

In contrast, Debre-Markos shows a consistent increase in precipitation across all scenarios, with a maximum increase of +36% under RCP8.5 by 2071–2100. Nekmte presents a minor decrease of up to -6% in two scenarios, while the other scenarios indicate either stability or a slight increase of +3%. These findings indicate that while some regions may experience a reduction in precipitation, others, particularly Debre-Markos, could see significant increases.

Table 3: Average Seasonal precipitation (mm) for Bega season in Historical period and two future period under RCP2.6 & RCP8.5 scenarios, with percentage change (% Decrease & % Increase &No-change)

No.	Stations	Historical Observation Data (1981-2005) Prec. (mm)	(2041-2070)		(2071-2100)	
			RCP2.6	RCP8.5	RCP2.6	RCP8.5
			Prec. (mm)		Prec. (mm)	
			% Change		% Change	
1	Roseires	37.2	39.8 6.99%	42.8 15.05%	45.1 21.24%	40.0 7.53%
2	Gonder	80.6	75.4 -6.45%	81.2 0.74%	77.4 -3.97%	81.4 0.99%
3	Bahr Dar	111.0	95.3 -14.14%	123.0 10.81%	101.3 -8.74%	131.5 18.47%
4	Kembolcha	103.5	93.6 -9.57%	93.1 -10.05%	109.4 5.70%	90.9 -12.17%
5	Debre-Markos	122.2	137.6 12.60%	146.7 20.05%	125.6 2.78%	166.3 36.09%
6	Nekmte	183.0	182.1 -0.49%	171.7 -6.17%	188.9 3.22%	183.0 0.0%

3.3. Z-Score Test (Indicator of the Numbers of Wet/Normal/Dry Years)

Table 4 shows Z-Score test results for the numbers of wet/normal/dry years in the historical observation duration of (1981-2005) and in the future projection durations of (2041-2070) (2071-2100) for the RCP2.6 & RCP8.5 scenarios. Table (4) also shows the percent of each of these years in the historical duration, and the percent change in their occurrence in future projection scenarios.

There is no clear trend for future projection changes in numbers of wet/normal/dry years in any of the scenarios; not in the increase/decrease of the numbers of years in each category, nor in the percent change. However, the smallest occurrence of any category was no less than 4 years in the 30-year duration, while the largest occurrence was at 16 years. The most repeated numbers of years in any category were (7, 8, 9, 10, 11, 12 & 13 years) which had repeated occurrences at (5, 6, 18, 14, 10, 7 & 5 times); respectively. These were followed by the occurrence of (16 years) only twice, and (4, 5, 6, 14 & 15 years) each of them occurring only once.

However, taking the averages for the 6 stations (at the bottom of Table 4) indicate a trend over the entire Blue Nile Basin (BNB). The average percentage of normal years in future projection scenarios seem around that of the historical data (around 37%) for RCP2.6 in the duration (2041-2070) and for both RCP2.6 & RCP8.5 in the duration (2071-2100), while RCP8.5 in (2041-2070) is much higher at 46%. Observation historical data averages show more wet years (at 35%) than dry years (at 28%). Meanwhile, future projection scenarios tend towards higher dry year percentages (30-38%, as compared to 28% in historical data) than wet years (24-30%, as compared to 35% in historical data). This may conclude that there is tendency for stability in the numbers of normal years, with tendency for some increase in dry years on the account of wet years in future projection simulations.

Table 4: Numbers of wet, normal and dry years based on Z-Score index for historical, and Future Periods under RCP2.6, RCP8.5 scenarios, with Percentage Changes (Decrease & Increase) in projection

Stations	Historical Observation Data (1981-2005)			2041-2070						2071-2100					
				RCP2.6			RCP8.5			RCP2.6			RCP8.5		
	No. of Years			No. of Years			No. of Years			No. of Years			No. of Years		
	*% of Duration			**% Change (Change from Hist.)			% Change (Change from Hist.)			% Change (Change from Hist.)			% Change (Change from Hist.)		
	wet	Norm	dry	wet	Norm	dry	Wet	Norm	dry	wet	Norm	dry	Wet	Norm	dry
Roseires	8	9	8	10	10	10	9	13	8	9	10	11	9	11	10
	32%	36%	32%	+1%	-3%	+1%	-2%	+7%	-5%	-2%	-3%	+5%	-2%	+1%	+1%
Gonder	8	12	5	10	11	9	10	8	12	9	12	9	9	10	11
	32%	48%	20%	+1%	-11%	+10%	+1%	-21%	+20%	-2%	-8%	+10%	-2%	-15%	17%
Bahr Dar	9	9	7	7	13	10	4	16	10	11	7	12	12	8	10
	36%	36%	28%	-13%	+7%	+5	-23%	+17%	+5%	+1%	-13%	+12%	+4%	-9%	+5%
Kembolcha	8	8	9	11	11	8	7	14	9	7	13	10	7	12	11
	32%	32%	36%	+5%	+5%	-10	-9%	+15%	-6%	-9%	11%	-2%	-9%	+8%	+1%
Debre-Marcos	12	5	8	9	12	9	9	15	6	8	13	9	9	9	12
	48%	20%	32%	-12%	+20%	-2	-18%	+30%	-12%	-21%	+23%	-2%	-18%	+10%	+8%
Nekmte	7	12	6	9	10	11	5	16	9	9	13	8	9	11	10
	28%	48%	24%	+2%	-15%	+13%	-11%	+5%	+6%	+2%	-5%	+3%	+2%	-11%	+9%
Average No. Years	9	9	7	9	11	10	7	14	9	9	11	10	9	10	11
Precentage (%) of Duration – Avg. % of 6 sts.	35%	37%	28%	30%	38%	32%	24%	46%	30%	30%	38%	32%	30%	32%	38%

* % of Duration = (No. of Wet/Norm/Dry Years) / (Historical duration)
** % Change = (% of simulation Duration) - (% of Historical Duration)

3.4. Annual Precipitation Concentration Indexes (PCI)

Table 5 presents the range and average annual Precipitation Concentration Index (PCI) for the studied stations, comparing historical (1981–2005) with future periods (2041–2070 and 2071–2100) under RCP2.6 and RCP8.5 scenarios. Extreme PCI values, which were excluded from average calculations, are detailed in the same Table, along with the classification of PCI strength. Extreme values were observed in two scenarios at Roseires station and in three scenarios at Kembolcha station. Historical PCI classifications ranged from 'moderate' to 'irregular,' with averages between 15% and 22%. Future projections indicate a shift toward 'strongly irregular' classifications for most stations, with PCI averages increasing to 16-31% across scenarios, reflecting greater precipitation variability. Extreme PCI values (e.g., 40-53%) were excluded in some cases, particularly under RCP8.5. Stations like Roseires and Kembolcha showed significant increases in PCI, while others like Debre-Markos remained 'irregular'. Nekmte transitioned from 'moderate' to 'irregular' in most future scenarios, except for 2071–2100 under RCP2.6, which stayed 'moderate.' Classification.

Table 5: Average annual Precipitation Concentration Index (PCI*) at the stations studied for the historical and the future durations under scenarios RCP2.6 & RCP8.5

No.	Station		PCI- Historical period (1981-2005)	(2041 – 2070)		(2071 – 2100)	
				PCI-RCP2.6	PCI-RCP8.5	PCI-RCP2.6	PCI-RCP8.5
1	Roseires	Range[1]	17-25%	20-34%	19-36%	20-36%	22-41%
		(excl. extremes)	(---)	(40%)	(---)	(---)	(47, 49, 53%)
		Average[2]	22%	26%	26%	26%	31%
		Description[3]	Strongly irregular	Strongly Irregular	Strongly Irregular	Strongly Irregular	Strongly Irregular
2	Gonder	Range[1]	16-28%	18-28%	17-32%	16-31%	19-32%
		(excl. extremes)	(---)	(---)	(---)	(---)	(---)
		Average[2]	20%	23%	24%	21%	25%
		Description[3]	Irregular	Strongly Irregular	Strongly Irregular	Strongly Irregular	Strongly Irregular
3	Bahr Dar	Range[1]	15-29%	19-27%	18-28%	18-27%	18-32%
		(excl. extremes)	(---)	(---)	(---)	(---)	(---)
		Average[2]	21%	23%	23%	22%	25%
		Description[3]	Strongly irregular	Strongly irregular	Strongly irregular	Strongly irregular	Strongly irregular
4	Kembolcha	Range[1]	13-26%	13-31%	16-41%	13-32%	17-36%
		(excl. extremes)	(---)	(---)	(53%)	(42%)	(47%)
		Average[2]	18%	23%	28%	22%	25%
		Description[3]	Irregular	Strongly irregular	Strongly irregular	Strongly irregular	Strongly irregular
5	Debre-Markos	Range[1]	13-21%	13-22%	14-23%	13-21%	14-28%
		(excl. extremes)	(---)	(---)	(---)	(---)	(---)
		Average[2]	17%	17%	19%	17%	20%
		Description[3]	Irregular	Irregular	Irregular	Irregular	Irregular
6	Nekmte	Range[1]	13-19%	14-20%	14-22%	13-19%	12-22%
		(excl. extremes)	(---)	(---)	(---)	(---)	(---)
		Average[2]	15%	16%	17%	15%	17%
		Description[3]	Moderate	Irregular	Irregular	Moderate	Irregular

*PCI: Uniform (< 10%:), Moderate (11-15%), Irregular (16-20%), Strongly Irregular (> 20%).
PCI: Range[1], Average[2] & Description[3] are determined excluding extreme values in the "Range", which are mentioned between parentheses in the cell below it.

3.5. Seasonal Precipitation Concentration Indexes (SPCI)
The Belg Season (Semi-Rainy)

Seasonal Precipitation Concentration Index (SPCI) for the Belg Season (Semi-Rainy) at the studied stations for the historical period (1981-2005) and the future projection durations of (2041–2070 & 2071-2100) under IPCC RCP2.6 & RCP8.5 emission scenarios is presented in **Table 6**.

SPCI in the historical data was 'strongly irregular' for Roseires station in Sudan and in future projections as well (historical: 16-33%, average 28%; future: 15-33%, averages 26.2-28%). In Ethiopia, Gonder and Bahr Dar stations shifted from "irregular" historical classifications (12-33%, averages 18.8-20%) to a mix of "moderate" and "irregular" in future projections (averages 15.6-19.5%). Kembolcha, Debre-Markos, and Nekmte stations, historically "moderate" (9-23%, averages 13.6-14.6%), largely maintained this classification in future scenarios, with averages ranging from 12.5% to 18.8%. No extreme SPCI values were excluded, ensuring robust analysis. The results highlight regional variability, with Sudan experiencing consistently high precipitation irregularity, while Ethiopian stations show moderate to irregular patterns, reflecting differing climate impacts under future scenarios.

Table 6: Average Seasonal Precipitation Concentration Index (SPCI*) for the Belg Season (Semi-Rainy) at the studied stations for the historical and future durations under RCP2.6 & RCP8.5 scenarios

No.	Station		SPCI Historical period (1981-2005)	(2041 – 2070)		(2071 – 2100)	
				SPCI-RCP2.6	SPCI-RCP8.5	SPCI-RCP2.6	SPCI-RCP8.5
1	Roseires	Range[1]	16-33%	16-33%	15-33%	17-33%	17-33%
		(excl. extremes)	(---)	(---)	(---)	(---)	(---)
		Average[2]	28%	26.2%	27%	26.2%	28%
		Description[3]	Strongly Irregular	Strongly Irregular	Strongly Irregular	Strongly Irregular	Strongly Irregular
2	Gonder	Range[1]	12-33%	11-29%	13-29%	12-29%	12-30%
		(excl. extremes)	(---)	(---)	(---)	(---)	(---)
		Average[2]	18.8%	15.6%	18%	16.8%	17.7%
		Description[3]	Irregular	Moderate	Irregular	Irregular	Irregular
3	Bahr Dar	Range[1]	12-32%	9-29%	11-30%	11-29%	11-31%
		(excl. extremes)	(---)	(---)	(---)	(---)	(---)
		Average[2]	20%	15.8%	19.5%	18%	19.2%
		Description[3]	Irregular	Moderate	Irregular	Irregular	Irregular
4	Kembolcha	Range[1]	9-22%	9-28%	10-29%	9-25%	9-32%
		(excl. extremes)	(---)	(---)	(---)	(---)	(---)
		Average[2]	13.6%	16%	18.2%	15.3%	18.8%
		Description[3]	Moderate	Irregular	Irregular	Moderate	Irregular
5	Debre-Markos	Range[1]	9-23%	9-20%	9-21%	8-18%	9-23%
		(excl. extremes)	(---)	(---)	(---)	(---)	(---)
		Average[2]	13.6%	12.5%	13.4%	12.6%	14.4%
		Description[3]	Moderate	Moderate	Moderate	Moderate	Moderate
6	Nekmte	Range[1]	9-22%	9-24%	11-24%	10-23%	10-27%
		(excl. extremes)	(---)	(---)	(---)	(---)	(---)
		Average[2]	14.6%	14.3%	16.1%	15.7%	15.6%
		Description[3]	Moderate	Moderate	Irregular	Moderate	Moderate

*SPCI: Uniform (< 10%:), Moderate (11-15%), Irregular (16-20%), Strongly Irregular (> 20%).
PCI: Range[1], Average[2] & Description[3] are determined excluding extreme values in the "Range", which are mentioned between parentheses in the cell below it.

The Kiremt Season (Rainy)

The analysis of the Seasonal Precipitation Concentration Index (SPCI) for the Kiremt Season across six stations in Sudan and Ethiopia is showed in **Table 7**. The results indicate a general shift from 'uniform' to 'moderate' SPCI values in future projections (2041–2070 and 2071–2100) under RCP2.6 and RCP8.5 scenarios. Historically, five stations exhibited 'uniform' SPCI, except for Kembolcha, which was 'moderate'. Future projections show increased precipitation concentration, particularly in northern and eastern stations, with the highest increases in Kembolcha (averaging up to 15% in 2041–2070 and 14.2% in 2071–2100). Meanwhile, southern and central stations, such as Nekmte and Debre-Markos, largely maintain 'uniform' values, except for Debre-Markos under RCP8.5 in 2071–2100. Notably, SPCI ranges widen in most stations, indicating increasing variability in precipitation distribution, which may have significant implications for hydrological stability and water resource management. The absence of extreme values suggests a consistent trend, but the increasing upper range in future scenarios, particularly under RCP8.5, highlights potential intensification in seasonal precipitation patterns.

Table 7: Average Seasonal Precipitation Concentration Index (SPCI*) for the Kiremt Season (Rainy) at the studied stations for the historical and the future durations under RCP2.6 & RCP8.5 scenarios

No.	Station		SPCI - Historical period (1981-2005)	(2041 – 2070)		(2071 – 2100)	
				SPCI-RCP2.6	SPCI-RCP8.5	SPCI-RCP2.6	SPCI-RCP8.5
1	Roseires	Range[1]	8-11%	9-14%	8-16%	9-17%	9-19%
		(excl. extremes)	(---)	(---)	(---)	(---)	(---)
		Average[2]	9.5%	11.3%	11%	11%	13%
		Description[3]	Uniform	Moderate	Moderate	Moderate	Moderate
2	Gonder	Range[1]	9-12%	9-14%	9-15%	9-15%	9-16%
		(excl. extremes)	(---)	(---)	(---)	(---)	(---)
		Average[2]	9.8%	11.2%	11.3%	11%	12.3%
		Description[3]	Uniform	Moderate	Moderate	Moderate	Moderate
3	Bahr Dar	Range[1]	8-12%	9-14%	9-13%	9-13%	9-15%
		(excl. extremes)	(---)	(---)	(---)	(---)	(---)
		Average[2]	9%	10.6%	10.5%	10.3%	11%
		Description[3]	Uniform	Moderate	Moderate	Moderate	Moderate
4	Kembolcha	Range[1]	9-14%	10-16%	11-24%	10-21%	11-21%
		(excl. extremes)	(---)	(---)	(---)	(---)	(---)
		Average[2]	11.5%	13.4%	15%	14%	14.2%
		Description[3]	Moderate	Moderate	Moderate	Moderate	Moderate
5	Debre-Markos	Range[1]	8-10%	8-12%	9-11%	9-11%	9-14%
		(excl. extremes)	(---)	(---)	(---)	(---)	(---)
		Average[2]	9.2%	9.8%	9.7%	9.4%	10.7%
		Description[3]	Uniform	Uniform	Uniform	Uniform	Moderate
6	Nekmte	Range[1]	8-9%	8-10%	8-11%	8-9.5%	8.5-11.5%
		(excl. extremes)	(---)	(---)	(---)	(---)	(---)
		Average[2]	8.8%	9%	9%	8.8%	9.4%
		Description[3]	Uniform	Uniform	Uniform	Uniform	Uniform

*SPCI: Uniform (< 10%:), Moderate (11-15%), Irregular (16-20%), Strongly Irregular (> 20%).
PCI: Range[1], Average[2] & Description[3] are determined excluding extreme values in the "Range", which are mentioned between parentheses in the cell below it.

The Bega Season (Dry)

Table 8 presents the Seasonal Precipitation Concentration Index (SPCI) for the Bega Season, comparing historical data (1981–2005) with future projections (2041–2070 and 2071–2100) under RCP2.6 and RCP8.5 scenarios. All stations, including Roseires, Gonder, Bahr Dar, Kembolcha, Debre-Markos, and Nekmte, exhibit "strongly irregular" SPCI classifications in both historical and future periods, with historical averages ranging from 14.2% to 23.8%. Future projections show similar trends, with averages ranging from 15.2% to 31.4%, indicating persistent high precipitation variability. Notably, Roseires maintains the highest SPCI averages (28.4–31.4%), reflecting extreme irregularity, while other stations like Kembolcha and Debre-Markos show slightly lower but still "strongly irregular" averages (15.2–19.9%). The exclusion of extreme values ensures robust analysis. Compared to **Table 5**, which showed a mix of "moderate" and "irregular" classifications for Ethiopian stations, this Table consistently classifies all stations as "strongly irregular," suggesting a more pronounced shift toward higher precipitation variability in the Bega season under future climate scenarios.

Table 8: Average Seasonal Precipitation Concentration Index (SPCI*) for the Bega Season (Dry) at the stations studied for the historical and future durations under RCP2.6 & RCP8.5 scenarios

No.	Station		SPCI - Historical period (1981-2005)	(2041 – 2070)		(2071 – 2100)	
				SPCI-RCP2.6	SPCI-RCP8.5	SPCI-RCP2.6	SPCI-RCP8.5
1	Roseires	Range[1]	17-33%	24-33%	17-33%	17-33%	17-33%
		(excl. extremes)	(---)	(---)	(---)	(---)	(---)
		Average[2]	31.1%	31.4%	30.7%	28.4%	29.3%
		Description[3]	Strongly Irregular	Strongly Irregular	Strongly Irregular	Strongly Irregular	Strongly Irregular
2	Gonder	Range[1]	12-31%	14-29%	16-31%	13-28%	14-31%
		(excl. extremes)	(---)	(---)	(---)	(---)	(---)
		Average[2]	21.4%	20.6%	20.8%	18.7%	19:4%
		Description[3]	Strongly Irregular	Strongly Irregular	Strongly Irregular	Strongly Irregular	Strongly Irregular
3	Bahr Dar	Range[1]	14-33%	15-31%	16-33%	13-30%	15-33%
		(excl. extremes)	(---)	(---)	(---)	(---)	(---)
		Average[2]	23.8%	23.3%	24.8%	21%	22.8%
		Description[3]	Strongly Irregular	Strongly Irregular	Strongly Irregular	Strongly Irregular	Strongly Irregular
4	Kembolcha	Range[1]	9-31%	10-32%	9-25%	9-32%	10-29%
		(excl. extremes)	(---)	(---)	(---)	(---)	(---)
		Average[2]	17.2%	15.3%	16.4%	15.2%	17.1%
		Description[3]	Irregular	Moderate	Irregular	Moderate	Irregular
5	Debre-Markos	Range[1]	9-33%	9-26%	12-32%	9-27%	9-29%
		(excl. extremes)	(---)	(---)	(---)	(---)	(---)
		Average[2]	18%	17.8%	19.9%	16.1%	19.7%
		Description[3]	Irregular	Irregular	Irregular	Irregular	Irregular
6	Nekmte	Range[1]	10-27%	11-28%	11-31%	11-25%	12-28%
		(excl. extremes)	(---)	(---)	(---)	(---)	(---)
		Average[2]	16.6%	17.9%	18.7%	16.3%	18.2%
		Description[3]	Irregular	Irregular	Irregular	Irregular	Irregular

*SPCI: Uniform (< 10%:), Moderate (11-15%), Irregular (16-20%), Strongly Irregular (> 20%).
PCI: Range[1], Average[2] & Description[3] are determined excluding extreme values in the "Range", which are mentioned between parentheses in the cell below it.

3.6. Comparison With Other Studies

The results obtained in this study are largely consistent with earlier applications of the ICTP-RegCM4 regional climate model to the Blue Nile Basin (BNB). Notably, RegCM4 was applied for the period 1982–2009 in previous studies, which observed a general decline in precipitation during the main rainy season (Kiremt), along with spatial heterogeneity in precipitation trends [11, 25]. Similarly, another study analyzing the 1981–2005 period reported considerable interannual variability and a gradual drying tendency, particularly under high-emission scenarios [26]. These findings are in broad agreement with the present study, which projects a decrease in annual and Kiremt season precipitation under both RCP2.6 and RCP8.5 scenarios.

Moreover, the observed increase in dry season (Bega) precipitation in this study aligns with emerging evidence from earlier research, which also noted a slight upward trend in Bega precipitation [27]. While there is general agreement on the increasing irregularity and concentration of precipitation, evidenced by higher PCI/SPCI values and a rise in dry years, some differences exist in the magnitude of changes across studies. For instance, the magnitude of Kiremt season reduction in this study (up to −14% under RCP8.5) is slightly higher than those reported in earlier works, potentially due to differences in emission scenarios, temporal resolution, bias correction methods, or spatial scales used in the analysis.

Importantly, these climatic shifts in the upstream BNB have broader implications for the entire Nile River system, including downstream regions such as the Nile Delta. One study highlighted significant concerns about the potential impacts of climate change on the coastal zone of the Nile Delta in Egypt [43]. Reduced and more erratic upstream precipitation, coupled with heightened interannual variability, could alter flow regimes and sediment transport, exacerbating vulnerabilities in the Delta; particularly under sea-level rise and salinization pressures. Thus, the findings reinforce the growing consensus that the Nile Basin is likely to face increasing climatic stress, from headwaters to delta, with notable shifts in seasonal precipitation patterns, reduced annual precipitation, and heightened temporal irregularity. These results further validate the use of RegCM4 as a reliable tool for regional climate projection in the Nile Basin, while also underscoring the urgent need for integrated, basin-wide climate adaptation and transboundary water governance mechanisms to address the cascading effects of climate change.

SUMMARY AND CONCLUSIONS

This study utilized simulation results from the regional climate model RegCM4.3 to project future precipitation changes in the Blue Nile Basin (BNB) for the periods 2041–2070 and 2071–2100 under the IPCC RCP2.6 and RCP8.5 emission scenarios. Bias correction was applied to the model's future projections using a correction function based on the historical observed dataset for period 1981–2005. The analysis included a comparison of the spatial distribution of seasonal precipitation across the BNB and six selected meteorological stations. Additionally, the study employed the Z-score index to evaluate the frequency of wet, normal, and dry years, as well as the annual and seasonal Precipitation Concentration Index (PCI/SPCI) to analyze the temporal distribution of monthly precipitation.

A comparison of the seasonal spatial-average future projection with historical precipitation data showed a general tendency for drier conditions as shown:

1) For Belg Season Projected precipitation changes range from –11% to –20% (2041-2070) and +1% to –34% (2071-2100), indicating a strong drying trend, especially under RCP8.5.

2) For Kiremt Season Precipitation is projected to decline by –5% to –7% for the near future period and –4% to –14% for the far future period, with consistent drying across both scenarios.

3) For Bega Season Precipitation is expected to change by –6% to +4% for near future period ,and +5% to +11% for far future period, showing a potential increase in precipitation during the dry season.

4) Annual precipitation is projected to decrease by –6% to –8% (2041-2070) and –2% to –15% (2071-2100).

5) Historical SPCI for the rainy (Kiremt) season was mostly uniform, but future projections show a shift toward moderate irregularity, indicating more uneven rainfall distribution. This can affect planting cycles and runoff patterns.

6) Annual PCI shifts from 'irregular/strongly irregular' historically to increasingly 'strongly irregular' in future scenarios due to seasonal precipitation imbalance and higher SPCI during Bega , where a small number of intense rainfall events can disproportionately affect the seasonal total despite overall lower rainfall volumes.

7) The results of Z-score Future projections show a stable proportion of normal years but an overall increase in dry years (28% historically to 28–38% in future scenarios) and a decrease in wet years from 35% historically to 24-35% in projections, indicating a shift toward more frequent dry conditions.

Overall, the study highlights significant spatial and temporal precipitation variability, emphasizing the need for coordinated transboundary water management and climate adaptation strategies among Ethiopia, Sudan, and Egypt. Further research is recommended to reduce uncertainties in future climate projections.

It is important to note that future projection simulation accounted for future emission scenarios but did not account for future SST (Sea Surface Temperature) scenarios. Also, Ninio and laNinia fenomena that are very powerfull in affecting the world climate require high resolution modilling scall that is not within the accuresy limit if the GCMs. This requires special consederation in modelling future projection scenarios.

The current study recommends that water resources management plans in the Blue Nile Basin riparian countries should account for the future expectation of less precipitation, more drier years, and less wetter years as projected by model simulations.

CONFLICT OF INTEREST

The authors have no financial interest to declare in relation to the content of this article.

REFERENCES

[1] M. M. Allam and E. A. B. Eltahir, "Water-energy-food nexus sustainability in the upper Blue Nile (UBN) basin," Front. Environ. Sci., vol. 7, no. JAN, p. 5, 2019. doi: 10.3389/fenvs.2019.00005.

[2] D. Conway and E. L. F. Schipper, "Adaptation to climate change in Africa: Challenges and opportunities identified from Ethiopia," Glob. Environ. Chang., vol. 21, no. 1, pp. 227–237, 2011. doi: 10.1016/j.gloenvcha.2010.07.013.

[3] IPCC, Impacts, Adaptation, and Vulnerability: Contribution of working group II to the fifth assessment report of the Intergovernmental Panel on Climate Change, no. March. Geneva: Intergovernmental Panel on Climate Change, 2014. [Online]. Available: http://www.citeulike.org/group/15400/article/13497155

[4] Z. Yihdego, A. Rieu-Clarke, and A. Cascão, "The Grand Ethiopian Renaissance Dam: An opportunity for collaboration and shared benefits in the Eastern Nile Basin," Water Int., vol. 42, no. 4, pp. 582–598, 2017. doi: 10.1080/02508060.2017.1329739.

[5] D. Whittington, J. Waterbury, and M. Jeuland, "The grand renaissance dam and prospects for cooperation on the eastern nile," Water Policy, vol. 16, no. 4, pp. 595–608, 2014. doi: 10.2166/wp.2014.011b.

[6] T. Beyene, D. P. Lettenmaier, and P. Kabat, "Hydrologic impacts of climate change on the Nile River Basin: Implications of the 2007 IPCC scenarios," Clim. Change, vol. 100, no. 3, pp. 433–461, 2010, doi: 10.1007/s10584-009-9693-0.

[7] E. Woldemariam and T. Ayenew, "Impacts of climate change on water resources in the Blue Nile Basin: A review," Environ. Syst. Res., vol. 9, no. 1, pp. 1–12, 2020. doi: 10.1186/s40068-020-00167-x.

[8] A. Swain, "Challenges for water sharing in the Nile basin: changing geo-politics and changing climate," Hydrol. Sci. J., vol. 56, no. 4, pp. 687–702, 2011. doi: 10.1080/02626667.2011.577037.

[9] D. P. van Vuuren et al., "The representative concentration pathways: An overview," Clim. Change, vol. 109, no. 1, pp. 5–31, 2011. doi: 10.1007/s10584-011-0148-z.

[10] F. J. Tapiador, A. Navarro, R. Moreno, J. L. Sánchez, and E. García-Ortega, "Regional climate models: 30 years of dynamical downscaling," Atmos. Res., vol. 235, p. 104785, 2020. doi: 10.1016/j.atmosres.2019.104785.

[11] M. A. H. Zaroug, F. Giorgi, E. Coppola, G. M. Abdo, and E. A. B. Eltahir, "Simulating the connections of ENSO and the rainfall regime of East Africa and the upper Blue Nile region using a climate model of the Tropics," Hydrol. Earth Syst. Sci., vol. 18, no. 11, pp. 4311–4323, 2014. doi: 10.5194/hess-18-4311-2014.

[12] K. Yersaw, M. Tadesse, and A. Gebeyehu, "Evaluation of CORDEX-Africa RCMs over the Katar Watershed, Ethiopia," Clim. Dyn., vol. 62, no. 3, pp. 1123–1141, 2024.

[13] B. Tadase, A. Kebede, and D. Fekadu, "Assessment of CORDEX regional climate models in the Arsi Zone, Ethiopia," Theor. Appl. Climatol., vol. 159, no. 1–2, pp. 45–60, 2024.

[14] B. Mathewos, T. Alemayehu, and M. Tesfaye, "Performance evaluation of regional climate models over the Omo Gibe Basin," Hydrol. Sci. J., vol. 68, no. 1, pp. 79–95, 2023.

[15] Z. Alemu and B. Woldeamlak, "Climate modeling over the Wabi Shebele Basin using CORDEX RCMs: Evaluation and projection," Environ. Model. Assess., vol. 28, no. 2, pp. 203–220, 2023.

[16] A. Girma, D. Teshome, and A. Dagne, "Evaluation of CORDEX RCMs in simulating climate over the Gidabo Basin, Ethiopia," J. Hydrometeorol., vol. 23, no. 4, pp. 1025–1040, 2022.

[17] A. A. Mohamed and M. El-Mahdy, "Observed climate trends and ENSO impacts on the Blue Nile Basin," Clim. Res., vol. 86, no. 2, pp. 187–200, 2021.

[18] A. A. Mohamed and M. El-Mahdy, “Trends in drought occurrence in the Blue Nile Basin from 1950 to 2018,” Int. J. Climatol., vol. 42, no. 6, pp. 3021–3035, 2022.

[19] D. Takele, H. S. Endris, and A. Asfaw, “Climate change impact on streamflow and water balance using RCA-GCM scenarios in Ethiopia,” Water, vol. 13, no. 19, p. 2687, 2021.

[20] S. Liersch, H. Koch, and F. F. Hattermann, “Management scenarios of the Grand Ethiopian Renaissance Dam and their hydrological impacts,” Sci. Total Environ., vol. 659, pp. 819–829, 2018.

[21] B. Koné, M. B. Sylla, I. Diallo, and F. Giorgi, “Improving regional climate simulations over West Africa: A comparative analysis of convective schemes in RegCM4,” Clim. Res., vol. 76, no. 2, pp. 117–134, 2018.

[22] W. Tefera, P. van der Zaag, and H. H. G. Savenije, “Downscaled climate projections for the Upper Blue Nile Basin and implications for water resources,” Climate, vol. 6, no. 4, p. 94, 2018.

[23] G. G. Haile, Q. Tang, G. Leng, and G. Jia, “Droughts in East Africa: Causes, impacts and resilience,” Earth-Science Rev., vol. 177, pp. 284–300, 2017.

[24] A. Ahmadalipour, H. Moradkhani, M. Svoboda, and J. Sheffield, “Century-scale drought risk in the United States: A localized approach,” Sci. Rep., vol. 7, no. 1, p. 5946, 2017.

[25] T. T. Zeleke, B. D. Yeshita, and F. M. Agidew, Evaluation of a Regional Climate Model for the Upper Blue Nile Region. Rijeka, Croatia: InTech, 2016. doi: 10.5772/64954.

[26] G. T. Gnitou, H. Tan, I. K. Nooni, and K. T. C. Lim Kam Sian, “Resolution-sensitive added value analysis of CORDEX-CORE RegCM4-7 past seasonal precipitation simulations over Africa using satellite-based observational products,” Remote Sens., vol. 14, no. 9, p. 2102, 2022. doi: 10.3390/rs14092102.

[27] S. A. Zahran, S. Mansour, and D. Ibrahim, “Assessing domain change sensitivity for regional climate model simulation (Reg-Cm4.3) at Blue Nile Basin,” Port-Said Eng. Res. J., vol. 28, no. 2, pp. 93–109, 2024.

[28] M. G. Tedla, M. Rasmy, K. Tamakawa, H. Selvarajah, and T. Koike, “Assessment of Climate Change Impacts for Balancing Transboundary Water Resources Development in the Blue Nile Basin,” Sustain., vol. 14, no. 22, p. 15438, 2022. doi: 10.3390/su142215438.

[29] S. G. Setegn, A. M. Melesse, D. Rayner, and B. Dargahi, “Climate change impact on water resources and adaptation strategies in the Blue Nile River Basin,” in Nile River Basin: Ecohydrological Challenges, Climate Change and Hydropolitics, vol. 9783319027203, New York: Springer, 2014, pp. 389–404. doi: 10.1007/978-3-319-02720-3_20.

[30] A. M. Melesse, W. Abtew, S. G. Setegn, and T. Dessalegne, “Hydrological Variability and Climate of the Upper Blue Nile River Basin,” in Nile River Basin, Dordrecht: Springer Netherlands, 2011, pp. 3–37. doi: 10.1007/978-94-007-0689-7_1.

[31] J. C. Woodward, M. G. MackLin, M. D. Krom, and M. A. J. Williams, “The River Nile: Evolution and environment,” in Large Rivers: Geomorphology and Management, (ed.); 2nd ed., Ed., Hoboken, NJ: John Wiley & Sons, 2022, pp. 388–432. doi: 10.1002/9781119412632.ch14.

[32] W. Abtew and S. B. Dessu, “Hydrology of the Blue Nile Basin Overview,” in The Grand Ethiopian Renaissance Dam on the Blue Nile, Cham: Springer, 2019, pp. 39–62. doi: 10.1007/978-3-319-97094-3_4.

[33] U. Kim and J. J. Kaluarachchi, “Climate change impacts on water resources in the upper Blue Nile River Basin, Ethiopia,” J. Am. Water Resour. Assoc., vol. 45, no. 6, pp. 1361–1378, 2009. doi: 10.1111/j.1752-1688.2009.00369.x.

[34] P. J. Akol, R. P. Z. Galla, S. Wanyonyi, and ..., “Nile Basin Climate,” in Nile Basin Water Resources Atlas, Entebbe: Nile Basin Initiative, 2016.

[35] M. S. Nashwan and S. Shahid, “Spatial distribution of unidirectional trends in climate and weather extremes in Nile river basin,” Theor. Appl. Climatol., vol. 137, no. 1–2, pp. 1181–1199, 2019. doi: 10.1007/s00704-018-2664-5.

[36] B. D. Enyew and G. J. Steeneveld, “Analysing the impact of topography on precipitation and flooding on the Ethiopian highlands,” J. Geol. Geosci., vol. 3, no. 2, 2014.

[37] P. E. Mellander, S. G. Gebrehiwot, A. I. Gärdenäs, W. Bewket, and K. Bishop, “Summer Rains and Dry Seasons in the Upper Blue Nile Basin: The Predictability of Half a Century of Past and Future Spatiotemporal Patterns,” PLoS One, vol. 8, no. 7, p. e68461, 2013. doi: 10.1371/journal.pone.0068461.

[38] D. S. Wilks, Statistical Methods in the Atmospheric Sciences, Fourth Edition. San Diego, CA: Academic Press, 2019. doi: 10.1016/C2017-0-03921-6.

[39] D. G. Sutton and V. Kempi, Constrained least-squares restoration and renogram deconvolution: A comparison with other techniques, vol. 38, no. 8. Dundee, UK, 1993. doi: 10.1088/0031-9155/38/8/003.

[40] P. B. Labade, S. B. Gavit, B. Ayare, and H. Bhange, “Analysis of rainfall variability using precipitation concentration index (PCI): A case study of Dapoli station,” Int. J. Res. Agron., vol. 7, no. 7S, pp. 433–436, 2024. doi: 10.33545/2618060x.2024.v7.i7sf.1116.

[41] D. Lamichhane et al., “Precipitation Concentration Variability and Its Association with Geographical Factors and ENSO Over Nepal from 1990 to 2020,” Earth Syst. Environ., pp. 1–17, 2024. doi: 10.1007/s41748-024-00461-6.

[42] K. Zhang, Y. Yao, X. Qian, and J. Wang, “Various characteristics of precipitation concentration index and its cause analysis in China between 1960 and 2016,” Int. J. Climatol., vol. 39, no. 12, pp. 4648–4658, 2019. doi: 10.1002/joc.6092.

[43] A., H. Gomma. "The Impact Of Climate Change On Coastal Cities In The Eastern Nile Delta Of Egypt." Journal of Al-Azhar University Engineering Sector, Vol. 17, 62, pp. 146-160.